

Coupled Chaotic Oscillators Composed of RC Circuits

Ayana Shimada[†], Hironori Kumeno[†], Yoko Uwate[†], Yoshifumi Nishio[†] and Jingmin Xin[‡]

[†] Tokushima University

2-1 Minami-Josanjima, Tokushima 770-8506, Japan

Phone: +81-88-656-7470

Email: {ayana,kumeno,uwate,nishio}@ee.tokushima-u.ac.jp

[‡] Xi'an Jiaotong University

28 Xianning Xilu, Xi'an, Shaanxi 710049, China

Phone: +86-29-8266-8802

Email: jxin@mail.xjtu.edu.cn

Abstract

In this study, we propose coupled chaotic oscillators composed of RC circuits. We carry out computer simulations and investigate chaotic behavior when the number of RC circuits are increased.

1. Introduction

Recently, many researchers have shown their interests in chaotic systems. Chaos has been investigated not only in engineering but also in various fields such as medicine, sociology and economics. In the field of electrical and electronic engineering, researchers have proposed various applications using chaos as chaos communications, chaos cryptosystem, chaos neural networks and so on. In order to realize chaotic engineering systems, it is important to investigate simple chaos-generating circuits. In our previous study, a simple chaotic oscillator using two RC circuits were proposed [1].

In this study, we propose coupled chaotic oscillators composed of RC circuits. By computer simulations, we investigate the chaotic behavior when the number of the coupled RC circuits are increased.

2. Circuit model

Figure 1 shows the circuit model. In this figure 15 chaotic oscillators, which was proposed in [1], are coupled via one-way coupling through simple comparators. An independent rectangular voltage source is connected only to the first oscillator and the voltage across one of the two capacitors in the previous stage of oscillators is inputted to the comparators in the next oscillator. Hence, the whole circuit consists of one rectangular voltage source, 30 comparators, 30 resistors, and 30 capacitors. Figure 2 shows the rectangular voltage waveform inputted to the first oscillator. V_S is the amplitude of the rectangular voltage and T is the period of the waveform.

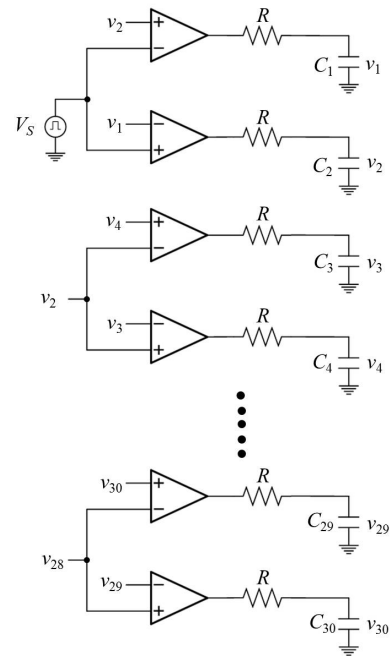


Figure 1: Circuit model.

The circuit equations are described as follows:

$$\begin{aligned}
 RC \frac{dv_1}{dt} &= \begin{cases} -v_1 - E & (v_2 > V_S) \\ -v_1 + E & (v_2 < V_S) \end{cases} \\
 RC \frac{dv_2}{dt} &= \begin{cases} -v_2 + E & (v_1 > V_S) \\ -v_2 - E & (v_1 < V_S) \end{cases} \\
 RC \frac{dv_n}{dt} &= \begin{cases} -v_n - E & (v_{n+1} > v_{n-1}) \\ -v_n + E & (v_{n+1} < v_{n-1}) \end{cases} \\
 RC \frac{dv_{n+1}}{dt} &= \begin{cases} -v_{n+1} + E & (v_n > v_{n-1}) \\ -v_{n+1} - E & (v_n < v_{n-1}) \end{cases} \quad (1) \\
 (n = 3, 5, 7, 9, \dots, 29)
 \end{aligned}$$

where E is the output voltage of the comparators, namely the DC supply voltage of the operational amplifiers. By using the

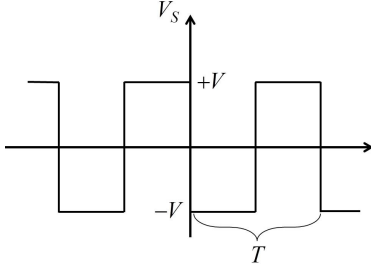


Figure 2: Rectangular voltage wave.

following variables and the parameters,

$$v_k = Ex_k, \quad t = RC\tau, \quad V_S = E\alpha, \quad T = RC\beta, \quad (2)$$

$$(k = 1, 2, \dots, 30)$$

we obtain the normalized circuit equations. Because the circuit equations are linear in each region, the rigorous solution of the circuit equations can be derived as follows:

$$x_1 = \begin{cases} (x_{10} + 1)e^{-\tau} - 1 & (x_2 > \alpha) \\ (x_{10} - 1)e^{-\tau} + 1 & (x_2 < \alpha) \end{cases}$$

$$x_2 = \begin{cases} (x_{20} - 1)e^{-\tau} + 1 & (x_1 > \alpha) \\ (x_{20} + 1)e^{-\tau} - 1 & (x_1 < \alpha) \end{cases}$$

$$x_n = \begin{cases} (x_{n0} + 1)e^{-\tau} - 1 & (x_{n+1} > x_{n-1}) \\ (x_{n0} - 1)e^{-\tau} + 1 & (x_{n+1} < x_{n-1}) \end{cases}$$

$$x_{n+1} = \begin{cases} (x_{(n+1)0} - 1)e^{-\tau} + 1 & (x_n > x_{n-1}) \\ (x_{(n+1)0} + 1)e^{-\tau} - 1 & (x_n < x_{n-1}) \end{cases} \quad (3)$$

$$(n = 3, 5, 7, 9, \dots, 29)$$

where α is a parameter corresponding to V_S , x_{10} , x_{20} and x_{n0} are initial values ($n = 3, 5, 7, 9, 11, \dots, 29$).

3. Simulation result

First, Fig. 3 and Fig. 4 show the attractors and their corresponding Poincaré maps, respectively, obtained from some chaotic oscillators. Comparing these figures, we can observe more complex attractors as the positions of the circuits increase.

Next, Figs. 5 and 6 are time waveforms. It is interesting that we can find essential difference between these two figures. Namely, in Fig. 5 chaotic waveforms are completely unsynchronized while in Fig. 6 chaotic waveforms of x_2 - x_{29} seem to almost synchronize in in-phase. The detailed analysis of these synchronization phenomenon is our important future research.

In order to evaluate chaotic features, we investigate the dispersion of the points on the Poincaré maps. Figure 7 shows

the average values of the standard deviation of the points for different α . We can see that the dispersion becomes larger as α increases.

Finally, we observe chaotic attractors and the Poincaré maps for different α values. Figure 8 shows chaotic attractors and Fig. 9 shows their corresponding Poincaré maps. As α increases, the size of the attractors clearly becomes large. However, only from these figures we cannot say whether if the complexity becomes large or small. Hence, further investigations are needed.

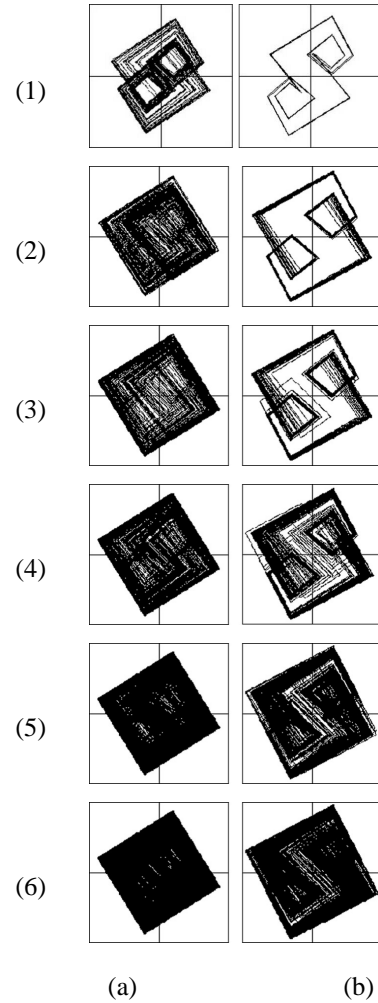


Figure 3: Chaotic attractor obtained from computer simulation ($\beta = 4.0$). (a) $\alpha = 0.097$ and (b) $\alpha = 0.180$. (1) x_1 - x_2 , (2) x_5 - x_6 , (3) x_{11} - v_{12} , (4) x_{17} - x_{18} , (5) x_{23} - v_{24} and (6) v_{29} - v_{30} .

4. Conclusions

In this study, we have proposed coupled chaotic oscillators composed of RC circuits. We carried out computer simula-

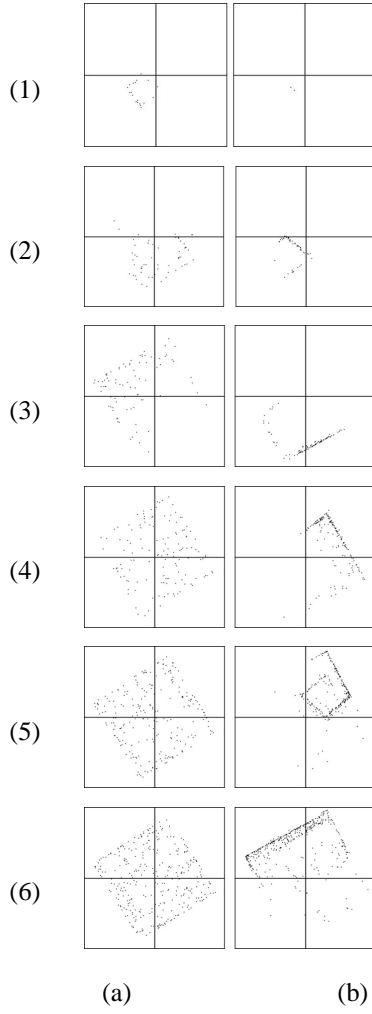


Figure 4: Poincaré map obtained from computer simulation ($\beta = 4.0$). (a) $\alpha = 0.097$ and (b) $\alpha = 0.180$. (1) x_1 - x_2 , (2) x_5 - x_6 , (3) x_{11} - v_{12} , (4) x_{17} - x_{18} , (5) x_{23} - v_{24} and (6) v_{29} - v_{30} .

tions and investigated chaotic behavior when the number of RC circuits were increased.

One of our future works is to carry out circuit experiments.

References

- [1] S. Masuda, Y. Uchitani and Y. Nishio, "Simple Chaotic Oscillator Using Two RC Circuits," Proc. of NCSP'09, pp. 89-92, 2009.

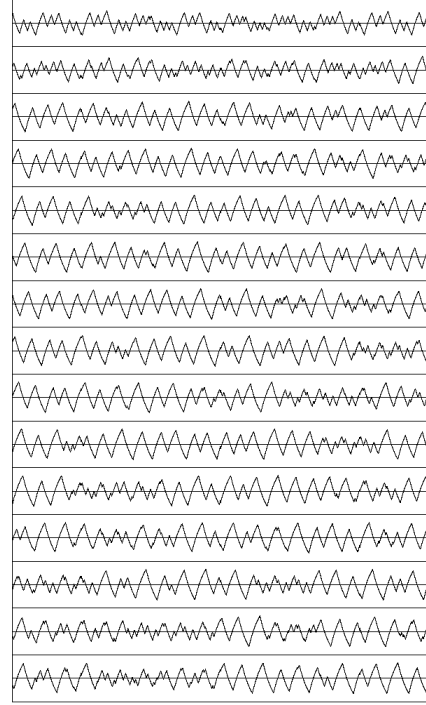


Figure 5: Time waveforms for $\alpha = 0.097$ and $\beta = 4.0$. From top $x_1, x_3, x_5, x_7, x_9, x_{11}, x_{13}, x_{15}, x_{17}, x_{19}, x_{21}, x_{23}, x_{25}, x_{27}, x_{29}$.

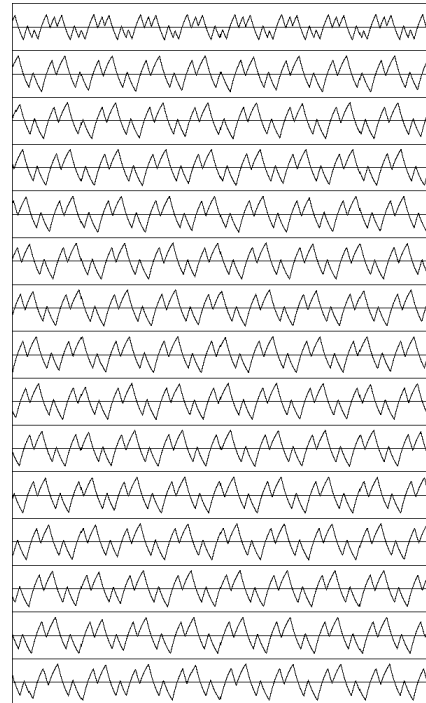


Figure 6: Time waveforms for $\alpha = 0.180$ and $\beta = 4.0$. From top $x_1, x_3, x_5, x_7, x_9, x_{11}, x_{13}, x_{15}, x_{17}, x_{19}, x_{21}, x_{23}, x_{25}, x_{27}, x_{29}$.

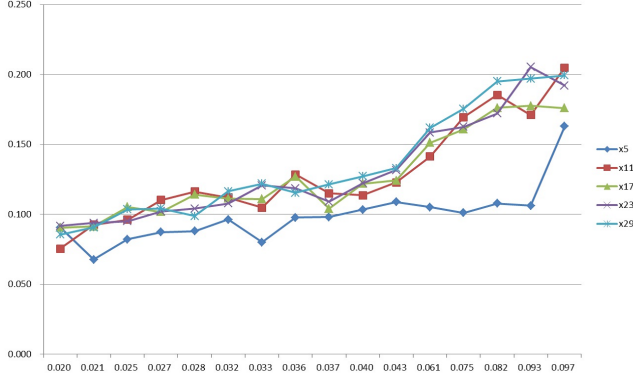


Figure 7: Change of standard deviation for different α . Only x_5 , x_{11} , x_{17} , x_{23} and x_{29} are shown.

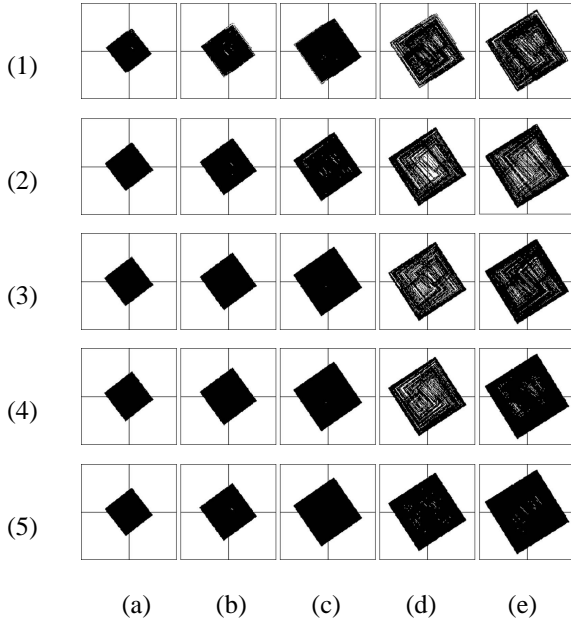


Figure 8: Chaotic attractors obtained from computer simulation ($\beta = 4.0$). (a) $\alpha = 0.027$, (b) $\alpha = 0.040$, (c) $\alpha = 0.061$, (d) $\alpha = 0.082$, and (e) $\alpha = 0.097$. (1) x_5 - x_6 , (2) x_{11} - x_{12} , (3) x_{17} - x_{18} , (4) x_{23} - x_{24} , and (5) x_{29} - x_{30} .

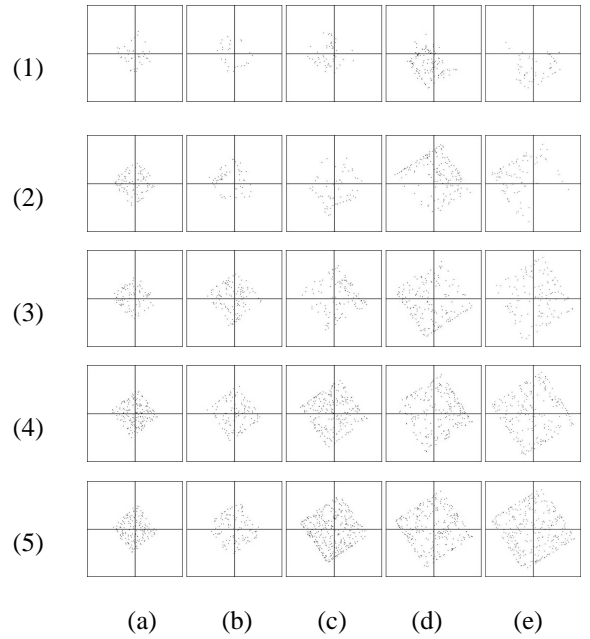


Figure 9: Poincaré maps obtained from computer simulation. ($\beta = 4.0$). (a) $\alpha = 0.027$, (b) $\alpha = 0.040$, (c) $\alpha = 0.061$, (d) $\alpha = 0.082$, and (e) $\alpha = 0.097$. (1) x_5 - x_6 , (2) x_{11} - x_{12} , (3) x_{17} - x_{18} , (4) x_{23} - x_{24} , and (5) x_{29} - x_{30} .